Study of Cogging Torque in Permanent Magnet Machines

C. Studer, Student Member A. Keyhani, SM
Department of Electrical Engineering
The Ohio State University
Columbus, OH 43210

T. Sebastian, Member S. K. Murthy, Member
Saginaw Steering Systems
Delphi
Saginaw, MI 48601

Abstract: Cogging torque is produced in a permanent magnet machine by the magnetic attraction between the rotor mounted permanent magnets and the stator. It is an undesired effect that contributes to the machines' output ripple, vibration, and noise. This paper analyzes various cogging torque minimization techniques as applied to a permanent magnet machine used in an electric power steering system. A six pole, eighteen slot, surface mounted, rare earth type, brushless permanent magnet machine is analyzed. The resultant cogging torque values are computed using a two and three-dimensional finite element analysis package.

Keywords: Brushless rotating machines, cogging torque, magnetic analysis, permanent magnet machines, rare earth materials, rotating machine nonlinear analysis, simulation.

Terminology:

Symbol	Description	Units
A	area	m^2
B	flux density	T
B_r	remanence	T
H	magnetic field intensity	A/m
ι	instantaneous current	A
P	number of poles	-
$\Re$	reluctance	H^{-1}
W'	co-energy	J
ϕ	magnetic flux	Wb
ϕ_g	air gap magnetic flux	Wb
μ_r	relative permeability	-
θ	rotor position	deg or rad
θ_{mech}	mechanical angle	deg or rad
τ_{cog}	cogging torque	N·m
τ_{cogpk}	peak value of cogging torque	N·m
ω	angular velocity	rad/sec

I. INTRODUCTION

Since the introduction of neodymium-iron-boron (NdFeB) magnetic materials [1, 2], brushless permanent magnet (PM) machines have found use in a wide variety of high performance applications. Various compositions of this magnetic material can produce larger flux densities than other PM materials previously used in brushless machines, even under more adverse demagnetization conditions [1, 2, 3].

These properties make NdFeB permanent magnets suitable for variable speed drive and high precision control applications.

Electric and hybrid-electric vehicles are currently being developed in order to better conserve energy. Energy conservation has become a goal for all technological fields. This implies that efficiency has become an important factor in electromechanical machine design.

Although PM machines are high performance devices, there are two torque components that affect their output performance. The first, called ripple torque, is produced from the harmonic content of the current and voltage waveforms in the machine [4, 5, 6]. The second, called cogging torque, is due to the physical structure of the machine [6, 7, 8, 9].

Cogging torque is produced, in a brushless PM machine, by the magnetic attraction between the rotor mounted permanent magnets and the stator teeth. It is the circumferential component of attractive force that attempts to maintain the alignment between the stator teeth and the permanent magnets.

Figure 1 displays two positions of a permanent magnet in relation to three stator teeth. The permanent magnet in figure 1 represents a single pole of a multi-pole machine. In figure 1a, the permanent magnet is aligned with the maximum amount of stator teeth. In this position, the circumferential components of force produced by the magnetic flux entering the stator teeth cancel. Thus, no net cogging torque is produced. For figure 1b, the rotor has been rotated in the counterclockwise direction. In this position, the circumferential components of force do not completely cancel. Thus, a net value of cogging torque exists. In this case, the cogging torque attempts to return the permanent magnet to that position displayed by figure 1a.

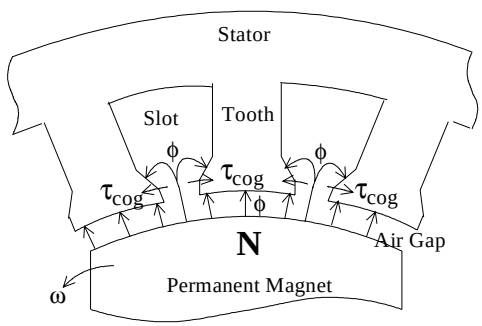

a. Net Cogging Torque Equal to Zero.

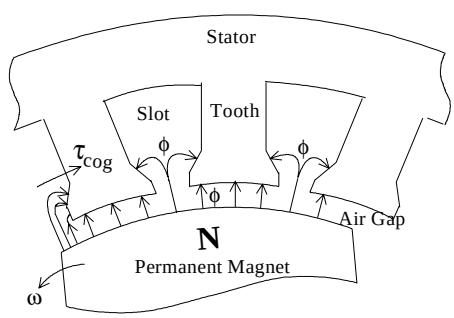

b. Net Cogging Torque Greater than Zero.
Fig. 1: Cogging Torque Production.

Cogging torque can be determined from the principle of virtual work [6, 7, 10, 11]:

$$\tau = \left.\frac{\partial W'(i,\theta)}{\partial \theta}\right|_{i=\text{constant}} \qquad (1)$$

For a brushless PM machine, torque consists of electromagnetic and reluctance components. Cogging torque defines the reluctance torque given by [6]:

$$\tau_{cog} = \sum_{1}^{P}\left(-\frac{1}{2}\phi_g^2\frac{d\Re}{d\theta}\right). \qquad (2)$$

One period of a typical cogging torque cycle is displayed by figure 2. To simplify the discussion of the cogging torque cycle, a salient pole stator and single bar magnet rotor are used.

Figure 2a displays the rotor aligned in an unstable detent position. A detent position is one in which the resultant cogging torque is zero. In this position, there is a maximum amount of air gap space between the rotor and stator. Thus, the maximum amount of air gap reluctance exists. Displacing the rotor from this position produces cogging torque that attempts to reduce the amount of air gap reluctance between the rotor and stator. Since the torque attempts to 'pull' the rotor away from this position, it is an unstable detent position.

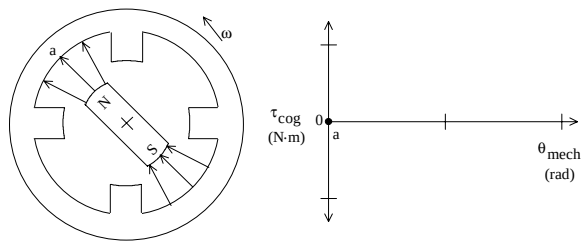

a. An Unstable Detent Position.

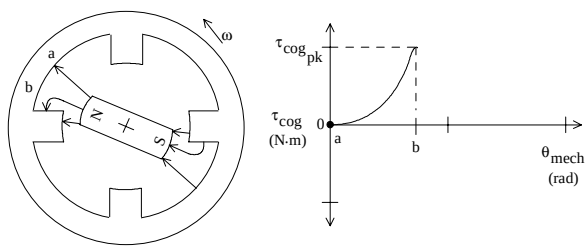

b. A Peak Cogging Torque Position.

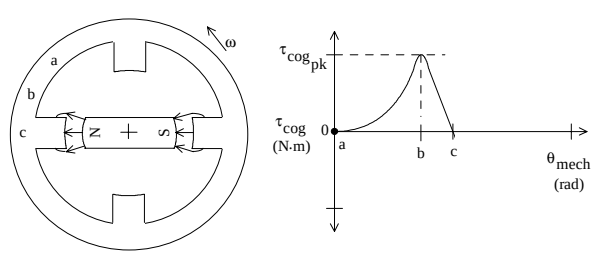

c. A Stable Detent Position.

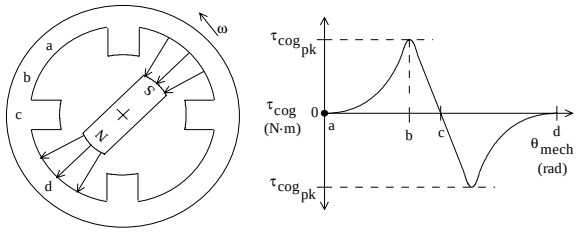

d. An Unstable Detent Position.

Fig. 2: One Period of a Typical Cogging Torque Cycle.

Assuming the rotor is rotating in the counterclockwise direction as shown, it reaches a position in which the circumferential attractive forces are maximum. As displayed by figure 2b, this position corresponds to the peak value of cogging torque produced by the machine. The cogging torque displayed by figure 2b 'pulls' the rotor to a stable detent position.

Figure 2c displays the rotor aligned in a stable detent position. Here, the air gap space and corresponding reluctance are minimized. Any displacement of the rotor from this position results in cogging torque which attempts to re-align the rotor to this position.

As the rotor rotates from position c to position d, the cogging torque completes one cycle as displayed by figure 2d. During this rotation, the cogging torque is negative. This implies the circumferential components of attractive forces are attempting to prevent the rotor from rotating in the counterclockwise direction. Thus, the cogging torque is attempting to 'pull' the rotor back to position c.

Cogging torque adds a ripple component to the desired constant output torque from the machine. This can produce vibration and noise which, in turn, reduces the performance of the machine.

II. COGGING TORQUE MINIMIZATION TECHNIQUES

Cogging torque minimization techniques have been analyzed for various electromechanical machines. In this paper, results for the following cases are provided:

(1) variation in magnet strength,
(2) variations in magnet arc length [5, 11],
(3) shifting magnetic poles [9-12],
(4) radial versus parallel magnetization [5, 13],
(5) rotor eccentricity,
(6) variations in the slot width [9],
(7) variations in the radial shoe depth,
(8) variations in yoke notch radii,
(9) permanent magnet skewing [7, 9, 11, 14-17], and
(10) permanent magnet overhang [9].

These methods are applied to a six pole, eighteen slot, surface mounted PM machine. The cross section of this machine is displayed by figure 3.

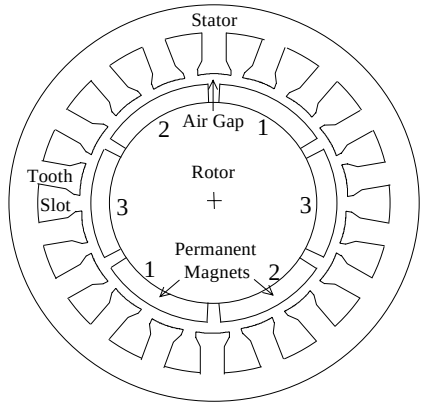

Fig. 3: Cross Section of a Six Pole, Eighteen Slot,
Surface Mounted Permanent Magnet Machine.

The machine and the minimization techniques are simulated using finite element analysis (FEA) software [18, 19]. Two-dimensional (2D) FEA [18] is used to simulate cases 1-8 above, whereas three-dimensional (3D) FEA [19] is used to simulate cases 9 and 10. For the 2D FEA cases previously listed, variations in magnet strength, magnet arc length, and slot width have the greatest effect on cogging torque. Resultant plots of cogging torque for these cases are therefore further analyzed in this paper. Results of the remaining 2D case studies are briefly summarized. The resultant cogging torque plots obtained from the 3D FEA are further discussed in this paper, although variations in the permanent magnet overhang produced negligible effects on cogging torque.

Referring to equation 2, cogging torque minimization techniques either reduce the rate of reluctance change with respect to rotor position, reduce the magnetic flux in the machine, or shift poles such that the cogging torque produced by the individual poles cancel one another. Nonetheless, when using a cogging torque minimization technique, either the construction of the machine becomes more complex or the performance of the machine is reduced.

A. Varying the Magnet Strength

The strength of a magnet corresponds to its flux producing capabilities. The magnetic flux produced by a permanent magnet is given by:

$$\phi = \int_A B \bullet dA \cdot \qquad (3)$$

Surface mounted NdFeB permanent magnets are used in this analysis. A typical demagnetization curve used to characterize NdFeB type permanent magnets is displayed by figure 4. The remanence and relative permeability are used to define the permanent magnet material by the software used to simulate the machine. Referring to figure 4, the magnet remanence is used to vary the flux density. This produces a proportional change in the amount of magnetic flux (equation 3) which, in turn, causes an appropriate change in the resultant cogging torque (equation 2).

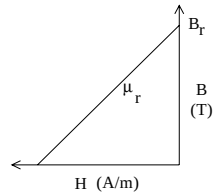

Fig. 4: Typical NdFeB Demagnetization Curve.

Varying the magnet strength with the remanence affects only the peak value of cogging torque. There should be no change in the shape of the cogging torque waveform since there is no change in the physical geometry of the machine.

Recall, the electromagnetic torque of the machine is directly proportional to the amount of magnetic flux produced by the permanent magnets. Thus, lowering the magnet remanence reduces the amount of magnetic flux within the machine thereby reducing the electromagnetic torque which, in turn, reduces the performance of the machine.

B. Varying the Magnet Arc Length

Referring to figure 1, cogging torque is produced when the magnetic flux from the leading edge of a permanent magnet enters a stator slot. This magnetic flux produces a net circumferential component of attractive force by entering the side of a stator tooth. Likewise, the magnetic flux from the trailing edge of a permanent magnet also produces cogging torque. Varying the magnet arc length directly affects the angular displacement between the leading and trailing edge and also affects the surface area of the permanent magnet. Both of these parameters affect the resultant cogging torque produced by the machine.

As the magnet arc length is reduced, the leading and trailing edge of the permanent magnet move closer to one another. This causes a shift in the circumferential components of attractive force developed by the permanent magnet edges. The resultant cogging torque may increase or decrease depending on the relationship between the magnet arc length and slot pitch [11].

As the magnet arc length is decreased, so is the surface area of the permanent magnet. This causes a decrease in the magnetic flux (equation 3) which, in turn, reduces the cogging torque produced by the machine (equation 2).

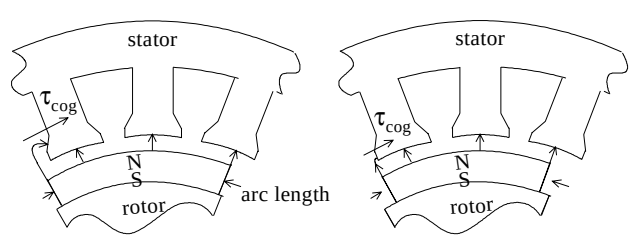

a. Arbitrary Arc Length b. Reduced Arc Length

Fig. 5: Variation in the Magnet Arc Length.

An arbitrary position for a single pole of a PM machine is displayed by figure 5. Figure 5a displays the cogging torque produced by the single pole having an arbitrary arc length. The decrease in arc length, displayed by figure 5b, shows a resultant decrease in the cogging torque for the same position of the rotor. Reducing the magnet arc length increases ripple torque, especially in trapezoidal PM machines [11]. Ripple torque, in general, is more dominant than cogging torque. It depends on the back electromotive force (EMF) which, in turn, is dependent on the magnet arc length. To minimize ripple torque, the magnet arc length should be maximized [5]. Thus, when varying the magnet arc length, a trade-off exists between cogging torque and ripple torque.

C. Varying the Slot Width

The effective air gap length of the machine depends on the slot width, which is also called the slot opening. The air gap flux depends on the effective air gap length of the machine. Likewise, cogging torque depends on the air gap flux, refer to equation 2. Thus, the slot width affects the cogging torque.

Reducing the slot width increases the arc length of the stator shoe at the air gap. Thus, the air gap flux has less of an opening in which to enter the slot region. Instead, a greater percentage of the air gap flux directly couples the stator at its shoes. Since less air gap flux enters the slot region, there is less flux entering the stator from the sides of the stator shoes. Thus, the circumferential components of force are reduced thereby, decreasing the cogging torque.

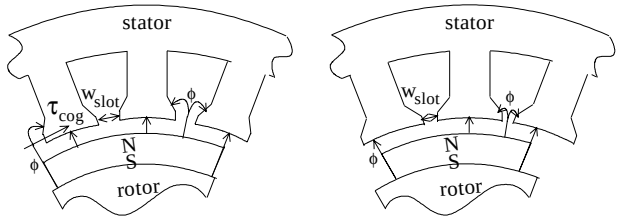

a. Arbitrary Slot Width b. Reduced Slot Width

Fig. 6: Variation in the Slot Width.

Figure 6 displays an arbitrary position of a single pole of a PM machine. Figure 6a displays the air gap flux entering the slot region for the machine having a nominal slot width. Figure 6b displays a reduction in air gap flux entering the slot region due to a decrease in the slot width.

D. Permanent Magnet Skewing

Skewing is a very common method used to reduce cogging torque in PM machines. It has been researched in depth both analytically [7, 17] and numerically [11, 14-16]. Skewing reduces the harmonic content in the slots by uniformly distributing the magnetic field [9, 14]. With respect to cogging torque, similar results occur whether the stator or the rotor-mounted permanent magnets are skewed. The disadvantage to skewing is that it creates magnetic forces in the axial direction of the machine. Skewing the stator has an additional disadvantage in that it increases the copper losses of the machine due to an increase in the stator winding length.

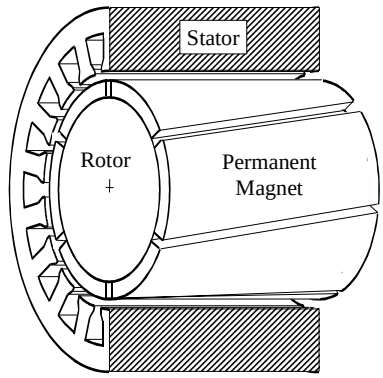

Fig. 7: Permanent Magnet Skewing.

Although 2D FEA can be used to analyze the effects of skewing [11], 3D FEA is used since it also accounts for magnetic leakage at both ends of the machine. Figure 7 displays the machine with the permanent magnets skewed by one slot pitch. Half of the stator has been removed to provide a better view of the rotor.

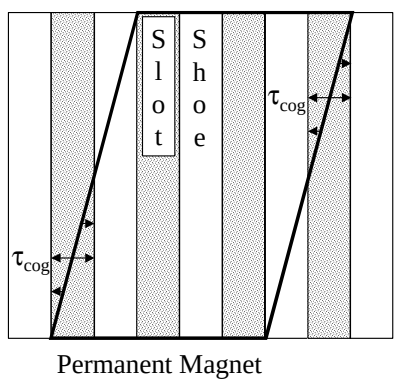

Fig. 8: Linear Model of Permanent Magnet Skewing.

Figure 8 displays a linear model of permanent magnet skewing. In this figure, the outline of a skewed magnet is shown superimposed on a linear stator segment. Also displayed are components of force from the permanent magnet edge that contribute to cogging torque. The net circumferential component of force is zero irregardless of the rotor position. Thus, skewing the permanent magnets by one slot pitch effectively eliminates cogging torque.

E. Permanent Magnet Overhang

Overhang exists if the axial length of the permanent magnets exceeds that of the stator, or vice versa. As the permanent magnet overhang increases, so does the flux density produced at the end of the machine. An increase in magnetic flux results (equation 3) which produces both circumferentially and axially directed magnetic forces. If there is an equivalent amount of overhang on each side of the machine, as displayed by figure 9, the axially directed magnetic forces cancel. The circumferentially directed magnetic forces contribute to the cogging torque in the machine. Thus, as the permanent magnet overhang increases, so does the resultant cogging torque [9].

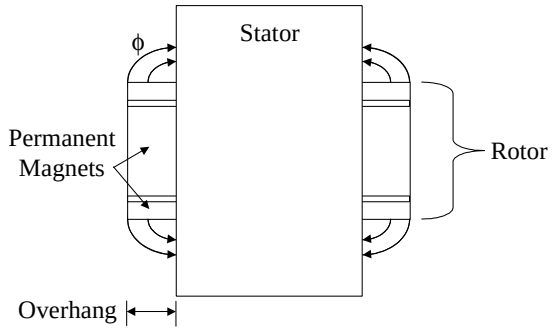

Fig. 9: Permanent Magnet Overhang.

III. RESULTS

For each analysis, the respective parameter is varied as discussed. Remaining parameters are set to their nominal values as given by table 1.

TABLE 1: NOMINAL VALUES FOR MACHINE PARAMETERS.

Magnet Remanence	1.25 T
Relative Permeability	1.07
Magnet Arc Length	58°
Slot Width	1.91 mm
Permanent Magnet Overhang	0 mm

One cycle of cogging torque is obtained for each analysis. For each cycle, the rotor position is varied from 0° to 20° in a counterclockwise direction from the initial position displayed by figure 3. In general, the rotor position is varied in increments of 0.3° for the 2D FEA. This provides relatively smooth plots even for the case studies where the shape of the cogging torque curve is dependent on the parameter being varied. For the 3D FEA, twelve arbitrary rotor positions are used to obtain each cogging torque curve. This was done to obtain a reasonable cogging torque curve without spending too much time on a single analysis due to the large computation time used in 3D FEA.

A. Varying the Magnet Strength

Figure 10 displays one cycle of cogging torque for a variation in magnet remanence. The magnet remanence is varied from 1.17 to 1.27 Tesla in increments of 0.01 Tesla. The relative permeability of the magnets is set equal to the nominal value given by table 1.

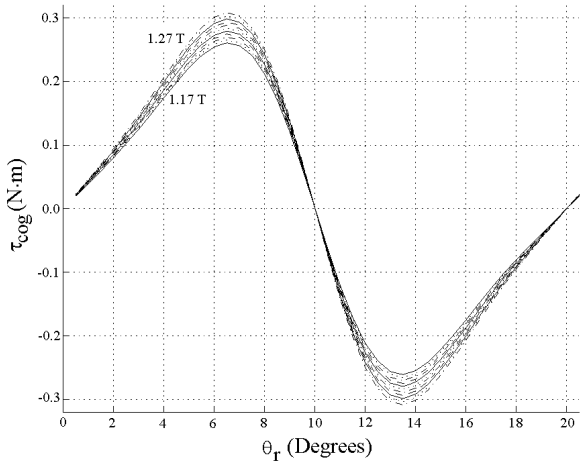

Fig 10: Cogging Torque Versus Rotor Position with Variations in Magnet Remanence.

As seen by figure 10, the peak value of cogging torque varies directly with the change in magnet remanence, while the shape of the curve remains unchanged. That is, the peak values of cogging torque, whose largest magnitude is approximately 0.31 N·m, occur at a rotor position of 6.5° and 13.5°. The largest magnitude of cogging torque occurs when the remanence is 1.27 T. From figure 10, the average value of cogging torque is zero Newton-meters.

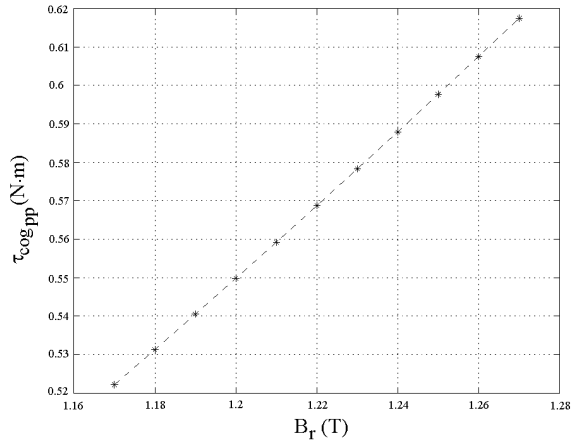

Fig 11: Peak-to-Peak Value of Cogging Torque Versus Magnet Remanence.

Figure 11 displays the peak-to-peak value of cogging torque versus the magnet remanence. For the given range, the ratio of peak-to-peak cogging torque versus magnet remanence is approximately 0.95 N·m per Tesla.

B. Varying the Magnet Arc Length

Figure 12 displays one cycle of cogging torque for a variation in magnet arc length. The magnet arc length is varied from 55° to 60° in one degree increments. The peak value of cogging torque increases

with an increase in magnet arc length. The largest magnitude of cogging torque is approximately 0.35 N·m. It occurs at a rotor position of approximately 7°, and 13°, when the magnet arc length is 60°.

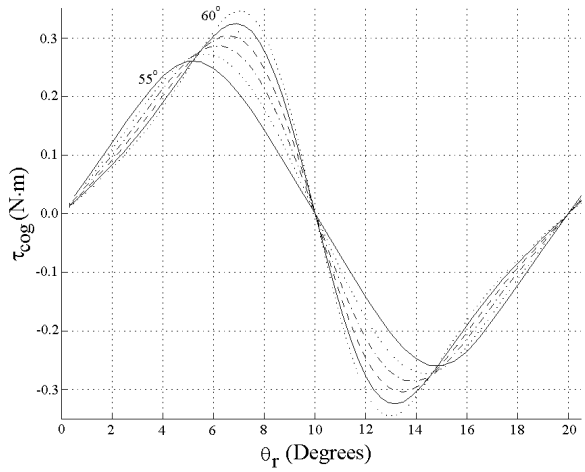

Fig 12: Cogging Torque Versus Rotor Position with Variations in Magnet Arc Length.

The shape of the cogging torque curve also changes with a variation in the magnet arc length. As the magnet arc length is increased, the peak value of cogging torque is developed at a rotor position closer to the stable detent position. The magnitude of cogging torque is also reduced near the unstable detent positions. Although the shape of the cogging torque curve changes, the average value of cogging torque remains zero Newton-meters.

The peak-to-peak value of cogging torque versus magnet arc length is displayed by figure 13. There is a nonlinear variation between the peak-to-peak value of cogging torque and the magnet arc length. The peak-to-peak value of cogging torque varied from 0.52 N·m to approximately 0.69 N·m for a five degree change in the magnet arc length.

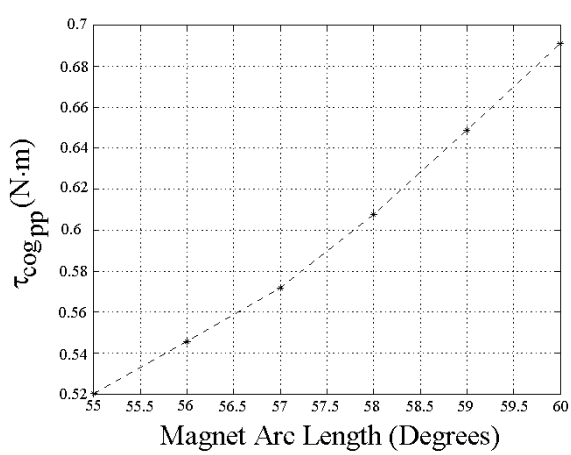

Fig 13: Peak-to-Peak Value of Cogging Torque Versus Magnet Arc Length.

C. Varying the Slot Width

Figure 14 displays one cycle of cogging torque for a variation in slot width. The slot width is varied from 1.5 to 2.9 millimeters in increments of 0.2 millimeters.

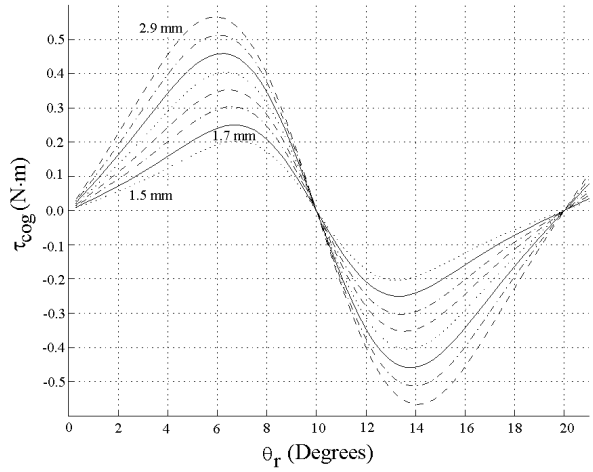

Fig 14: Cogging Torque Versus Rotor Position with Variations in Slot Width.

The peak value of cogging torque, from figure 14, varies directly with the change in slot width. There is a small change in the shape of the curve as well. As with the other cases analyzed thus far, the average value of cogging torque remains zero throughout this analysis.

The maximum value of cogging torque, which is approximately 0.56 N·m, occurs when the slot width is 2.9 mm. The peak value of cogging torque occurs at different rotor positions depending on the value of slot width. From figure 14, there is approximately a one degree change in the rotor position, where the peak value of cogging torque occurs, as the slot width is varied from 1.5 to 2.9 mm.

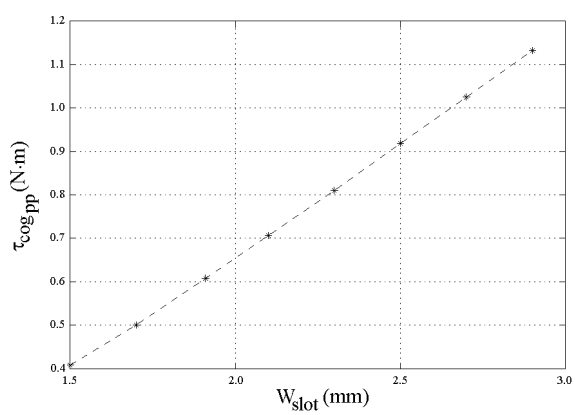

Fig 15: Peak-to-Peak Value of Cogging Torque Versus Slot Width.

Figure 15 displays the peak-to-peak value of cogging torque versus the slot width. For the given range, the ratio of peak-to-peak cogging torque versus slot width is approximately 0.52 N·m per millimeter.

D. Comparison Between 2D and 3D FEA Results

The previously analyzed cases involved 2D FEA in which no consideration was given to skewing or to magnetic end effects. The cogging torque curve are obtained for a 3D model of the machine having nominal parameter values, given in table 1. This allows comparison of 3D FEA results with 2D FEA results for the nominal machine. Figure 16 displays the resultant cogging torque curves.

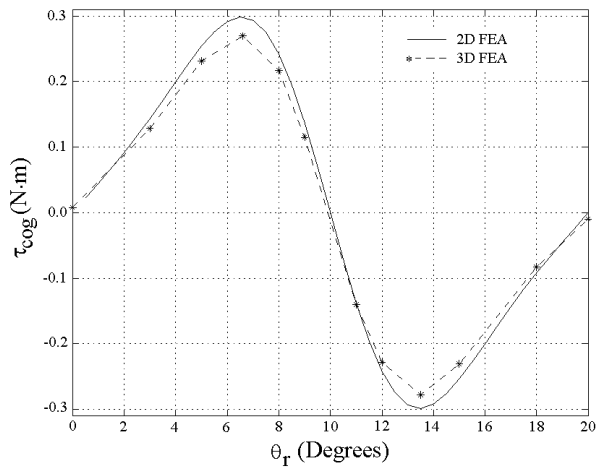

Fig 16: Comparison of Cogging Torque Versus Rotor Position Between 2D FEA and 3D FEA for the Nominal Model.

The cogging torque curves for the nominal machine using both the 2D and 3D FEA are similar. The detent and peak values occur at the same rotor position, and both curves approximate one another near the detent positions. The magnitudes between each curve differ by approximately 0.03 N·m. The cogging torque curve for the nominal machine obtained using 3D FEA has the smaller magnitude.

This trend is similar to that analyzed for a four pole machine [20]. In this analysis, the 3D FEA results more closely approximated the measured cogging torque curve. Like the results obtained in this paper, the largest magnitude of cogging torque occurred with the 2D FEA. The remaining 3D FEA results are compared with the nominal 3D case displayed by figure 16.

E. Permanent Magnet Skewing

Figure 17 displays one cycle of cogging torque for two cases of magnet overhang. In each case, the permanent magnets are skewed by one slot pitch (20°).

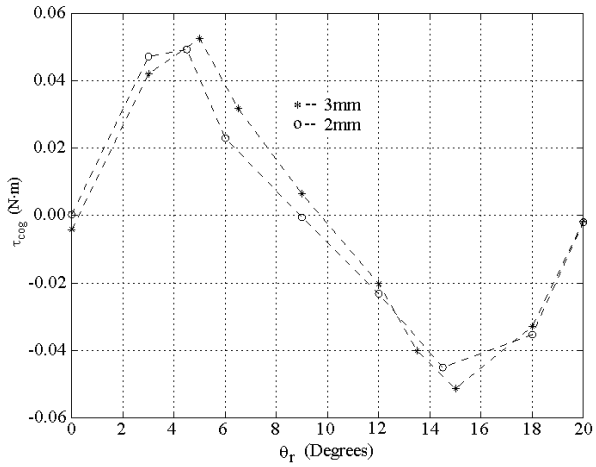

Fig 17: Cogging Torque Versus Rotor Position for One Slot Pitch of Skew and Variations in Magnet Overhang.

From figure 17, the peak value of cogging torque increases as the magnet overhang increases. The peak value of cogging torque is approximately 0.05 N·m. It occurs when the magnet overhang is 3 millimeters. Comparing figure 17 with figure 16, skewing the permanent magnets by one slot pitch has decreased the peak value of cogging torque by approximately one fifth. This decrease accounts for the PM overhang in the skewed model.

Figure 18 displays the peak-to-peak value of cogging torque versus the magnet overhang for the two cases that have been analyzed. For the two cases, the ratio of peak-to-peak cogging torque versus magnet overhang, when one slot pitch of skew exists, is approximately 9.6×10^{-3} N·m per mm.

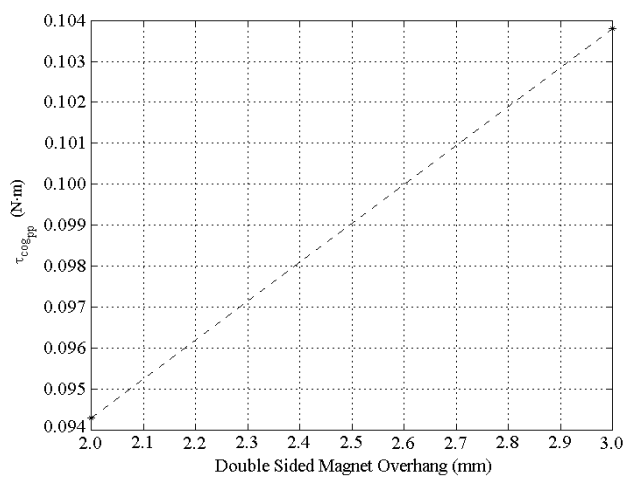

Fig 18: Peak-to-Peak Value of Cogging Torque Versus Magnet Overhang with One Slot Pitch of Skew.

F. Permanent Magnet Overhang

Figure 19 and 21 display one cycle of cogging torque for a variation in single and double sided PM overhang respectively. Comparing the two plots, the magnitude of cogging torque depends on the amount of PM overhang while the shape of the cogging torque waveform does not. Variations in the double sided PM overhang have a greater effect on the magnitude of cogging due to the increased magnetic field at both ends of the machine.

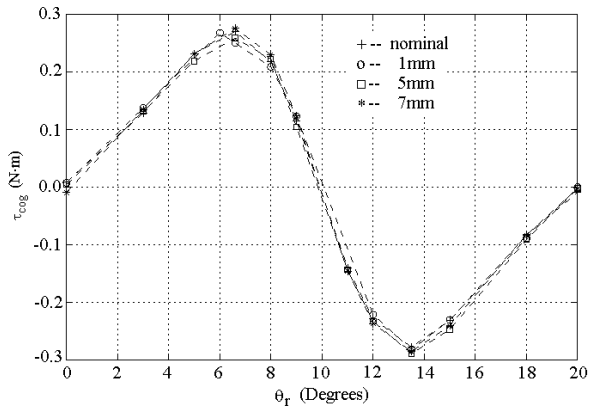

Fig 19: Cogging Torque Versus Rotor Position with Variations in Single Sided Magnet Overhang.

The peak value of cogging torque occurs at a rotor position of approximately 6.5° and 13.5° for both the single and double sided PM overhang cases. The largest magnitude of cogging torque, for the single sided PM overhang case, is approximately 0.28 N·m. It occurs when the single sided PM overhang is 7 millimeters. For the double sided PM overhang case, the largest magnitude of cogging torque is approximately 0.31 N·m (negative peak value). It occurs when the single sided PM overhang is 3 millimeter.

The -2 millimeter PM overhang displayed by figure 21 implies the stator overhangs the rotor by 2 millimeters at each end. Thus, comparing the stator overhang with the nominal case, as the stator overhang increases, the magnitude of cogging torque decreases.

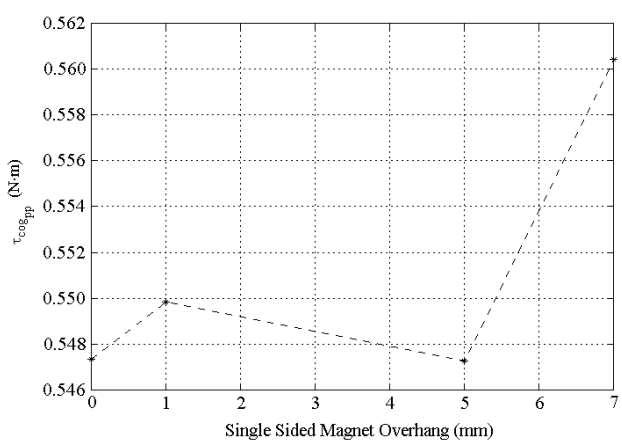

Fig 20: Peak-to-Peak Value of Cogging Torque

Versus Single Sided Magnet Overhang.

Figure 20 and 22 display the peak-to-peak value of cogging torque versus the permanent magnet overhang for the single and double sided PM overhang cases respectively. From these plots, the double sided PM overhang has a greater effect on the peak-to-peak value of cogging torque than the single sided PM overhang.

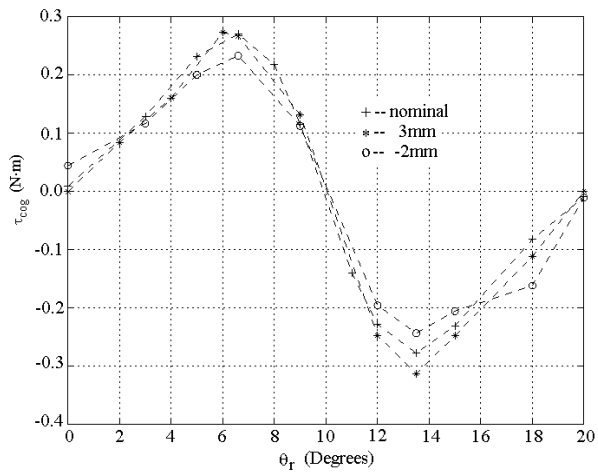

Fig 21: Cogging Torque Versus Rotor Position with
Variations in Double Sided Magnet Overhang.

For the given range, there is approximately a $7x10^{-3}$ N·m change in the peak-to-peak value of cogging torque for a 7 mm change in the single sided PM overhang. In the double sided PM overhang case, there is approximately a 0.013 $N{\cdot}m_{pp}$ change in cogging torque per millimeter change in the permanent magnets overhang when the magnets overhang the stator. There is approximately a 0.069 $N{\cdot}m_{pp}$ change in cogging torque per millimeter change in the PM overhang when the stator overhangs the rotor.

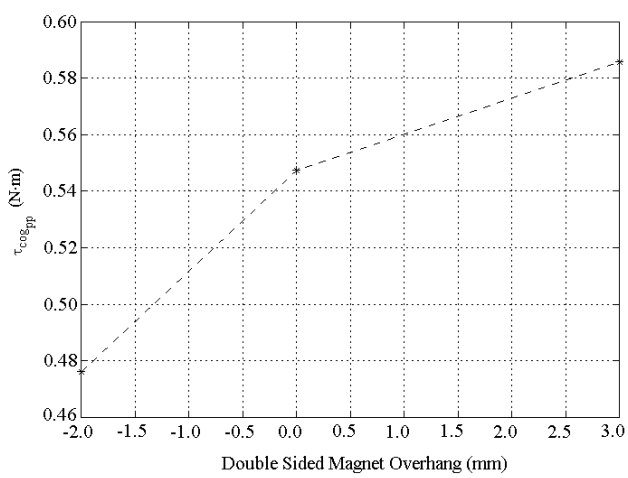

Fig 22: Peak-to-Peak Value of Cogging Torque
Versus Double Sided Magnet Overhang.

G. Summary of Cogging Torque Case Studies

TABLE 2: RESULTS OF THE COGGING TORQUE MINIMIZATION TECHNIQUES.

Analysis	Range	$\Delta\tau_{cogpk}$	τ_{cog} Shift
Magnet strength	1.17 - 1.27 T	≈ 0.95 N·m per T	none
Magnet arc length	55° - 60°	0.52 - 0.69 N·m	≈ 2°
Single pole pair offset	≥ 0.5° filler	0.012 N·m for 1.5° offset	< 1° for 1.5° offset
Double pole pair offset	≥ 0.5° filler	0.04 N·m for 3° offset	≈ 2° for 3° offset
Magnetization (radial vs. parallel)	not applicable	0.102 N·m (radial > parallel)	< 1°
Rotor eccentricity	Δ0.5 mm axial center	0.013 N·m	none
Slot width	1.5 - 2.9 mm	≈ 0.515 N·m per mm	≈ 1°
Radial shoe depth	0.5 - 1.5 mm	0.016 N·m	none
Yoke notches (0°,120°,240°)	r_{notch} = 0.75, 1, 2, 3, 4 mm	0.001 N·m	none
Yoke notches (0°,100°,200°)	r_{notch} = 0.75, 1, 2, 3, 4 mm	0.003 N·m	none
Nominal (2D vs. 3D)	Not applicable	0.029 N·m (2D > 3D)	none
PM overhang	0 - 7 mm	0.007 N·m	none

(single sided)			
PM overhang (double sided)	-2 - 3 mm	0.055 N·m	none
Magnet skew	1 slot pitch 0 - 3 mm	0.005 N·m	none

Table 2 summarizes the results for the cogging torque minimization techniques previously listed in section II. As previously stated, variations in the magnet strength, magnet arc length, slot width, and skewing produce the greatest effect on cogging torque, as analyzed in this paper.

IV. CONCLUSIONS

An analysis of various cogging torque minimization techniques as applied to a six pole, eighteen slot, surface mounted, rare earth type, permanent magnet, brushless machine was performed. A two and three dimensional finite element analysis package was used in the simulation.

The minimization techniques, from this paper, having the greatest effect on the resultant cogging torque are variations in magnet strength, magnet arc length, slot width, and permanent magnet skewing. Each of these cases has a significant effect on the magnitude of cogging torque. Variations in the magnet arc length and slot width also affects the shape of the cogging torque waveform.

V. ACKNOWLEDGMENTS

This work is supported in part by Delphi Steering Systems.